# VEGF-A has a critical, nonredundant role in angiogenic switching and pancreatic β cell carcinogenesis

Masahiro Inoue,[1,4,5] Jeffrey H. Hager,[1,4] Napoleone Ferrara,[2] Hans-Peter Gerber,[2] and Douglas Hanahan[1,3]

[1]Department of Biochemistry & Biophysics, Diabetes and Comprehensive Cancer Centers, University of California at San Francisco, San Francisco, California 94143
[2]Department of Molecular Oncology, Genentech Inc., South San Francisco, California 94080
[3]Correspondence: dh@biochem.ucsf.edu
[4]These authors made equal contributions to this work.
[5]Present address: Department of Tumor Biochemistry, Osaka Medical Center for Cancer and Cardiovascular Disease, Osaka 537-8511, Japan

## Summary

**In the RIP1-Tag2 mouse model of pancreatic islet carcinoma, angiogenesis is switched on in a discrete premalignant stage of tumor development, persisting thereafter. Signaling through VEGF receptor tyrosine kinases is a well-established component of angiogenic regulation. We show that five VEGF ligand genes are expressed in normal islets and throughout islet tumorigenesis. To begin dissecting their contributions, we produced an islet β cell specific knockout of VEGF-A, resulting in islets with reduced vascularity but largely normal physiology. In RIP1-Tag2 mice wherein most oncogene-expressing cells had deleted the VEGF-A gene, both angiogenic switching and tumor growth were severely disrupted, as was the neovasculature. Thus, VEGF-A is crucial for angiogenesis in a prototypical model of carcinogenesis, whose loss is not readily compensated.**

## Introduction

It is now widely accepted that tumor growth depends on angiogenesis, the formation of new blood vessels. Without the concomitant growth of new blood vessels (or a means to effectively co-opt existing capillary networks), tumors cannot expand beyond a minimal size, invade locally, or metastasize to distant sites. Angiogenesis, like many biological systems, is under both positive and negative control, regulated by a balance between pro- and antiangiogenic molecules. A considerable body of evidence supports the proposition that angiogenesis is initiated by an angiogenic switch that is tripped when the balance shifts in favor of the angiogenesis inducers (Hanahan and Folkman, 1996). Elucidation of the molecular components of the angiogenic switch will further our understanding of this exquisitely regulated process, and consequently suggest new therapeutic targets.

Genetically engineered mouse models of cancer have proven useful in characterizing multistage carcinogenesis (Van Dyke and Jacks, 2002), in particular for assessing acquired capabilities and the mechanisms that effect them, one of which is induction of angiogenesis in the quiescent normal vasculature of tissues (Hanahan and Weinberg, 2000). The RIP-Tag mouse is one such model (Hanahan, 1985), wherein pancreatic islet carcinogenesis unfolds as a result of expression in pancreatic islet β cells of the SV40 early region, which encodes potent large and small T antigen (Tag) oncoproteins. In one particularly well-characterized line (RIP1-Tag2), T-antigen is expressed in the developing embryonic pancreas without apparent effect, until 4–5 weeks of age, when β cell hyperproliferation ensues. A subset of the resultant hyperplastic and dysplastic islets progress during the next 5 weeks into "angiogenic islets," with a demonstrably activated vasculature (Folkman et al., 1989). A few weeks later, a few (5–10) encapsulated adenomas emerge, of which about 25% progress into invasive carcinomas. Angiogenic islets can be detected both morphologically (in tissue sections and in physically isolated islets), by their red color and evident blood islands consequent to microhemorrhaging, and functionally, by their ability to elicit endothelial cell migration, proliferation, and tube formation in an in vitro collagen gel bioassay involving coculture of dispersed capillary endothelial cells and isolated pancreatic islets (Folkman et al., 1989).

### SIGNIFICANCE

**An ongoing challenge for cancer biology and for development of therapeutic strategies that target tumor angiogenesis is to ascertain the relative contributions of the multitude of angiogenesis regulators that are typically expressed in tumors. Here we demonstrate, in a strict genetic test, that the angiogenesis inducer VEGF-A has a critical, apparently nonredundant role in the induction of tumor angiogenesis in a prototypical pathway of multistage carcinogenesis, despite expression of multiple angiogenic regulatory genes. Notably, no robust, VEGF-A null tumors arose that would have been indicative of functionally compensatory angiogenic signaling. These results support the focus on VEGF-A and its receptors as a therapeutic target, and suggest that long-term abrogation of VEGF signaling may not necessarily result in "resistant," VEGF-A independent tumors.**

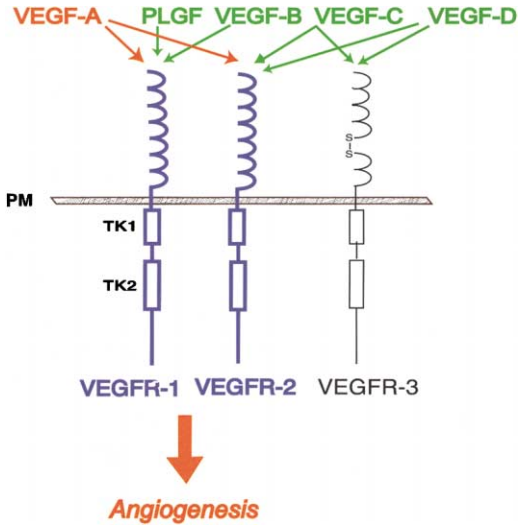


**Figure 1.** The complex and overlapping signaling potential of the VEGF family of angiogenesis regulators

VEGF-A, -B, -C, -D and PLGF bind as indicated to VEGFR-1 and/or VEGFR-2, receptor tyrosine kinases whose expression largely restricted to endothelial cells. In adults, the related VEGFR-3 is expressed primarily in lymphatic vessels and can demonstrably regulate lymphangiogenesis; it may also have a role in developmental angiogenesis. The specificity of VEGF ligand-receptor interactions depicted here has been recently reviewed by Shibuya et al. (1999), among others.

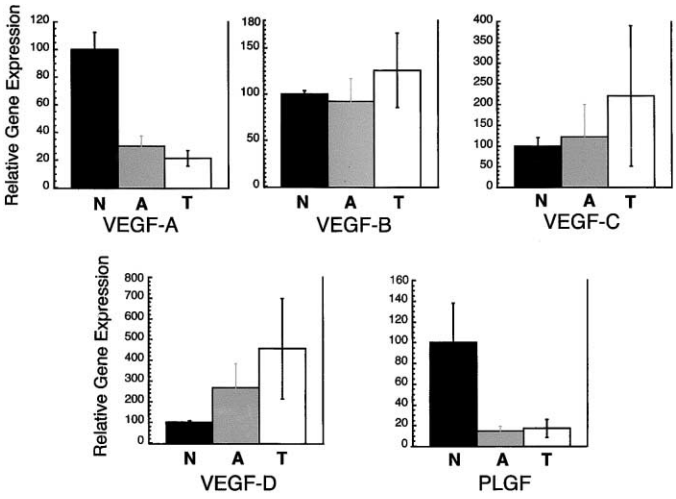


**Figure 2.** All known members of VEGF ligand family are expressed in normal islets and throughout islet β cell tumorigenesis

Real-time RT-PCR gene expression analysis of VEGF family members in normal, nontransgenic islets (N), angiogenic islets (A), and tumors (T) from RIP1-Tag2 mice. Data are shown as relative expression compared to normal islets (100%), and were standardized for GAPDH levels.

A prominent angiogenesis signaling system has been broadly implicated in a variety of cancers, and in particular in this model. VEGF-A (a.k.a. VEGF) signals through two transmembrane tyrosine kinase receptors selectively expressed on endothelial cells; VEGF-A has been implicated as a proliferation, migration, and survival factor for endothelial cells, as well as a molecule capable of eliciting neovascularization in a variety of ex vivo and in vivo angiogenesis bioassays (Ferrara, 1999). VEGF-A is expressed in the β cells of normal islets and at all stages of RIP1-Tag2 tumorigenesis (Christofori et al., 1995). Likewise, the VEGF-A receptors, VEGFR-1 and VEGFR-2, are constitutively expressed in normal islet and Rip1-Tag2 tumor vasculature (Christofori et al., 1995). This constancy of expression suggests that if VEGF-A activity is important in this tumorigenesis pathway, other modes of regulation must be involved. Indeed, our recent work has implicated MMP-9 in the proteolytic release of ECM-bound VEGF-A, thereby increasing its bioavailability with resultant activation of angiogenesis (Bergers et al., 2000).

Functional studies have implicated VEGF signaling in angiogenesis and tumor growth in the RIP1-Tag2 model. Treatment of RIP1-Tag2 mice with SU5416 (Vajkoczy et al., 1999), a small molecule inhibitor of the VEGF receptors, results in a significant reduction (>90%) in the number of angiogenic islets and in substantially reduced tumor burden (Bergers et al., 2000). Similar results were obtained when an adenovirus vector was used to deliver a soluble form of VEGFR-1 (sflt) that binds PLGF, VEGF-A, and VEGF-B (Compagni et al., 2000). Together, these results suggest that VEGF ligands play important role in RIP1-Tag2 angiogenesis and tumorigenesis, a hypothesis we have begun to address.

## Results

The pronounced effects of functionally inhibiting VEGF receptor signaling implicate VEGF ligands in the RIP1-Tag2 tumorigenesis pathway. In previous work we have shown that VEGF-A is expressed constitutively in the pathway, and we have implicated its "mobilization" from the ECM by a protease, MMP-9, in angiogenic switching (Bergers et al., 2000). However, the other VEGF family members have all been documented to have angiogenic regulatory activity, and could in principle function as critical regulators of angiogenesis in this tumor pathway. The complex and overlapping nature of the VEGF signaling axis is depicted in Figure 1. In short, all VEGF family members have the potential to modulate angiogenesis through the binding and activation of VEGFR-1 and/or VEGFR-2. To determine whether any of the other 4 known members of the VEGF family were expressed, we carried out real-time quantitative RT-PCR (Taqman) for VEGF-A, -B, -C, -D and PLGF on RNAs isolated from normal, nontransgenic islets, and from angiogenic islets and end-stage tumors from RIP1-Tag2 mice (Figure 2). As expected from our previous studies, VEGF-A is expressed in all three stages examined. Likewise, the other 4 VEGF family members are expressed at significant levels in all three stages. Interestingly, the mRNAs for VEGF-A and PLGF are downregulated in the angiogenic stages. The significance of this downregulation is unclear, but it does not result in loss of expression of VEGF protein in the case of VEGF-A. Immunohistochemical analyses of the protein have revealed VEGF-A to be readily detected in normal islets and in all stages of islet tumorigenesis (Bergers et al., 2000; Christofori et al., 1995) as well as in medium conditioned by angiogenic islets and tumors in organ culture (Christofori et al., 1995). The quantitative PCR results reveal that all of the known VEGF genes are expressed in this pathway, raising the possibility that VEGF-receptor mediated angiogenesis might be governed by some or all of the ligands they encode. We chose to

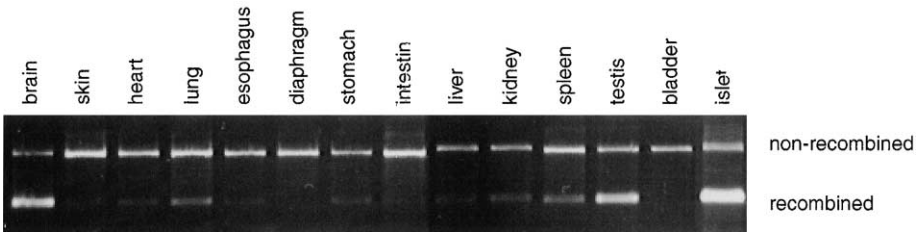


**Figure 3.** Cre-mediated recombinational deletion of the VEGF-flox allele in RIP-Cre mice

The PCR primers used span the floxed region of the VEGF-A gene such that the PCR product of the recombined allele is smaller than that of the nonrecombined allele. As expected, significant recombination was observed in intact isolated islets. In addition to islets, brain and testis showed appreciable recombination, while lung, kidney, and spleen exhibited low but detectable recombination. There was no apparent phenotypic consequence to the VEGF gene loss in these other tissues, which were not targets of oncogene expression and resultant neoplasia.

begin a genetic dissection of the functional contribution of these angiogenic factors through the use of a tissue specific knockout of the VEGF-A gene, a strategy motivated by the embryonic lethality of the germline knockout of this gene (Carmeliet et al., 1996; Ferrara et al., 1996).

### Absence of VEGF-A attenuates development of pancreatic islet vasculature

The bacteriophage Cre/loxP site-specific recombination system was used to generate a β cell specific VEGF-A null allele. We used a well-characterized transgenic mouse strain (Postic et al., 1999) in which Cre recombinase is under transcriptional control of the rat insulin promoter (RIP-Cre), in combination with a VEGF-A/loxP mouse line (Gerber et al., 1999), wherein exon 3 of the VEGF-A gene is flanked by loxP recombination sites ("floxed"). β cell expression of the RIP-Cre transgene commences during embryogenesis and elicits recombination in approximately 85% of β cells of adult mice (Kulkarni et al., 1999). The floxed VEGF allele has been shown to be a very efficient target of Cre recombinase in multiple tissues (Gerber et al., 1999). RIP-Cre;*Vegf*$^{fl/+}$ and RIP-Cre;*Vegf*$^{fl/fl}$ mice were generated, and both were found to be fully viable and indistinguishable in weight and size from *Vegf*$^{fl/fl}$ control littermates. In the presence of Cre recombinase, exon 3 of the floxed VEGF allele was deleted in the majority of the islet β cells, as revealed by two assays. Genomic DNA derived from isolated islets showed clear Cre dependent recombination, as evidenced by a PCR-based assay. Recombination was also detected in brain, testis, and, to a lesser extent, lung, kidney, and spleen (Figure 3), without apparent phenotypic effect. We suspect that this lack of phenotype in non-islet organs reflects Cre expression in only a small subset of cells in these tissues, and/or that the VEGF-A gene is not expressed in these cell types in normal, nonpathological conditions. The efficiency of recombinational deletion was also evident in pancreatic islet sections stained with an anti-VEGF antibody. VEGF protein levels were comparable in islets from *Vegf*$^{fl/fl}$ (Cre$^{-}$) and RIP-Cre;*Vegf*$^{fl/+}$ mice. In contrast, islets from RIP-Cre;*Vegf*$^{fl/fl}$ mice showed markedly reduced immunoreactivity in most islet cells, although a few scattered cells with apparently wild-type VEGF levels were observed (Figures 4J–4L). These VEGF-positive cells likely represent cells of the other endocrine lineages and/or β cells with nonrecombined floxed VEGF alleles.

To assess the effects of substantially reducing the number of VEGF-expressing cells on islet morphology and vascularization, pancreatic sections from RIP-Cre;*Vegf*$^{fl/+}$ and RIP-Cre;*Vegf*$^{fl/fl}$ mice were analyzed by staining with Hematoxylin and Eosin (H&E), by immunostaining with an antibody recognizing the endothelial marker PECAM (CD31), and by i.v. perfusion with a fluorescently labeled lectin (Figure 4). There was no obvious alteration in overall islet mass in either RIP-Cre;*Vegf*$^{fl/+}$ or RIP-Cre;*Vegf*$^{fl/fl}$ mice. However, H&E staining suggested a modest decrease in the density of β cells in RIP-Cre;*Vegf*$^{fl/fl}$ islets (Figures 4A–4C). Moreover, a pronounced reduction in blood vessel density was observed in RIP-Cre;*Vegf*$^{fl/fl}$ islets, as evidenced by CD31 and lectin staining (Figures 4D–4I). Lectin perfusion further revealed that the vasculature in VEGF-A deficient islets exhibited decreased branching in comparison to normal control islets (Figures 4G–4I). Despite these perturbations in islet vascularization, glucose homeostasis was normal, and there was no indication of diabetes (data not shown). The RIP-Cre;*Vegf*$^{fl/fl}$ mice did show a modest delay in their response to a bolus intraperitoneal injection of glucose (a glucose tolerance test), indicating a mild defect in glucose sensing or insulin secretion (data not shown). The viability and general normality of the RIP-Cre;*Vegf*$^{fl/fl}$ mice, along with the demonstration of substantial reduction in islet VEGF expression, afforded the possibility to assess the β cell specific knockout of VEGF in the context of islet carcinogenesis in compound RIP-1-Tag2;RIP-Cre;*Vegf*$^{fl/fl}$ mice.

### VEGF-A is critical for angiogenic switching and tumor growth

Beginning at 5–6 weeks of age, hyperplastic/dysplastic islets in RIP1-Tag2 mice undergo angiogenic switching, evidenced by capillary dilation, sprouting, and microhemorrhaging; the latter produces the "red islet" phenotype, which is attributed both to blood leaking from the tips of new capillary sprouts and to poor integrity of the neovasculature. Notably, normal islets are highly vascularized and, as such, angiogenic islets are not scored by relative increases in vessel density, but rather by these other qualities of pathological angiogenesis. To assess the role of VEGF-A in the angiogenic switch, the angiogenic islets (macroscopically red in color) were quantified at a defined endpoint of 10 weeks of age (Figure 5A), much as previously described (Bergers et al., 1999, 2000). The number of angiogenic islets in RIP1-Tag2;*Vegf*$^{fl/fl}$ mice lacking Cre recombinase ($n = 7$) ranged from 12 to 30 (avg. = 21.1), similar to traditional Rip1-Tag2 controls. In contrast, RIP1-Tag2/Cre;*Vegf*$^{fl/fl}$ littermates ($n = 4$) typically had only 1 angiogenic islet, with some mice evidencing none by this assay ($P < 0.05$). RIP1-Tag2/Cre *Vegf*$^{fl/+}$ (heterozygous knockout) mice ($n = 4$) had a similar number of angiogenic islets to control RIP1-Tag2;*Vegf*$^{fl/fl}$ (Cre$^{-}$) mice, suggesting that

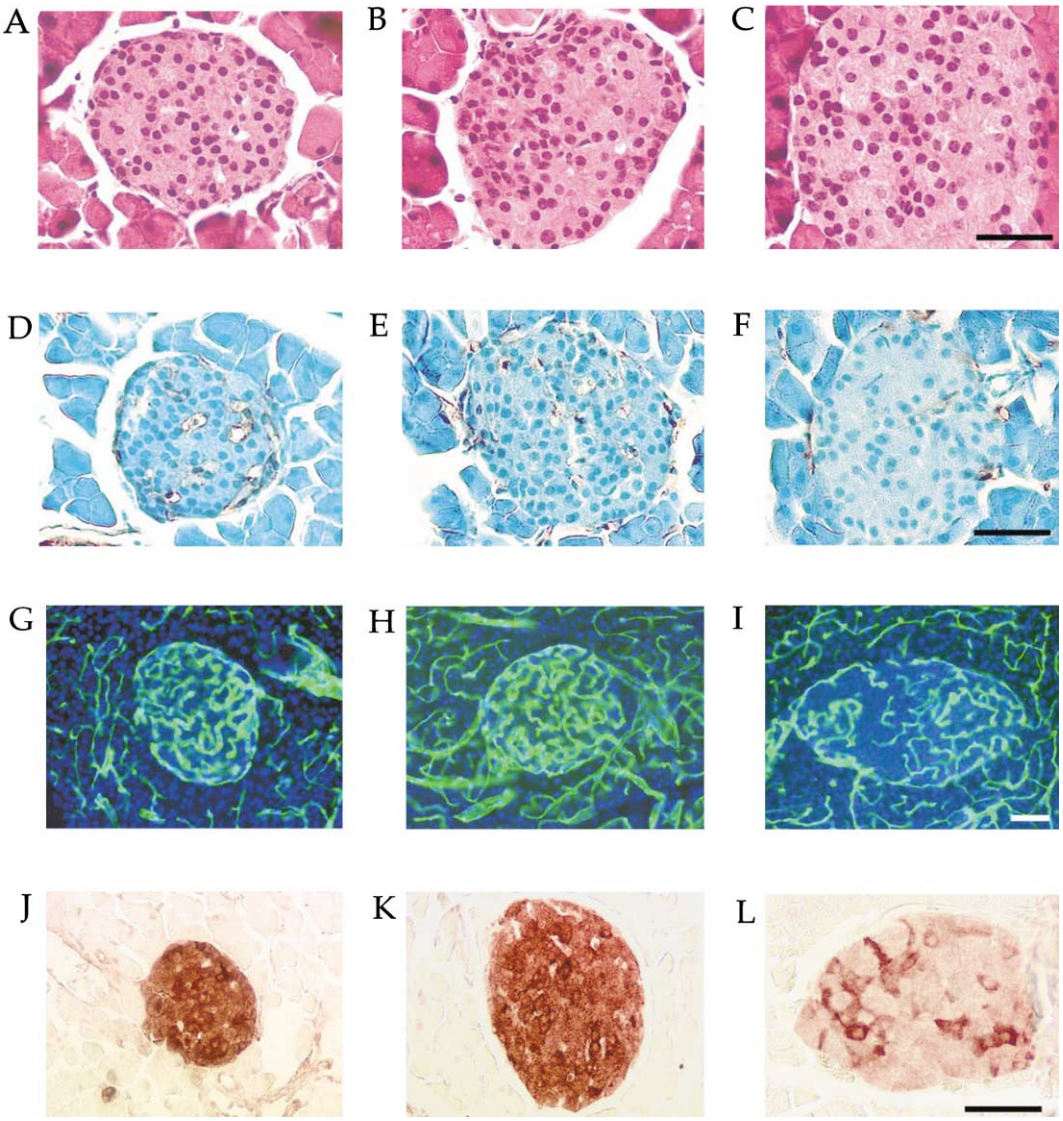


**Figure 4.** VEGF-A is involved in normal islet vascularization

**A–C:** Hematoxylin and Eosin staining reveals a slight increase in the cytoplasmic/nuclear ratio of Rip-Cre;*Vegf*$^{fl/+}$ (**B**) and Rip-Cre;*Vegf*$^{fl/fl}$ (**C**) islets when compared to wild-type islets (**A**).
**D–F:** CD31 (PE-CAM) was used to visualize the islet capillaries; wild-type (**D**) and Rip-Cre;*Vegf*$^{fl/+}$ (**E**) islets are indistinguishable. In contrast, the islets of Rip-Cre;*Vegf*$^{fl/fl}$ mice had a marked decrease CD31 immunoreactivity, which is most evident in the interior of the islets (**F**).
**G–I:** Blood vessel staining by lectin perfusion revealed the vascular density to be significantly decreased in Rip-Cre;*Vegf*$^{fl/fl}$ (**I**) but not in Rip-Cre;*Vegf*$^{fl/+}$ islets (**H**) compared to the control islets (**G**).
**J–L:** VEGF immunostaining assessed the effects of the cre-mediated recombination on VEGF-A gene expression. Wild-type (**J**) and Rip-Cre;*Vegf*$^{fl/+}$ islets (**K**) exhibited strong homogeneous staining, while Rip-Cre;*Vegf*$^{fl/fl}$ islets (**L**) had a considerably reduced level of staining. The images presented are representative of the analysis of three mice and at least 10 islets per mouse.

one functional allele of VEGF-A is sufficient for angiogenic islet formation.

Next we assessed tumor number and tumor burden at a defined endpoint of 12-week-old animals (Figures 5B and 5C). In control RIP1-Tag2;*Vegf*$^{fl/fl}$ (Cre$^{-}$) animals (n = 16), tumor number ranged from 2 to 10, as it did in RIP1-Tag2/Cre;*Vegf*$^{fl/+}$ mice carrying a nonfloxed wild-type VEGF allele that was not susceptible to inactivation by Cre-mediated recombination. In contrast, RIP1-Tag2/Cre;*Vegf*$^{fl/fl}$ mice (n = 7) had 0 to 3 tumors detectable by gross pathology (Figure 5B). When tumor burden was assessed in these same animals, an even more remarkable difference emerged: RIP1-Tag2/Cre;*Vegf*$^{fl/fl}$ mice had a mean collective tumor volume of 3 mm$^3$, whereas control RIP1-Tag2;*Vegf*$^{fl/fl}$ mice had an average burden of 63.5 mm$^3$ ($P < 0.05$) (Figure 5C). Interestingly, while RIP1-Tag2/Cre;*Vegf*$^{fl/+}$ (heterozygous knockout) mice (n = 9) had no significant difference in tumor number (or angiogenic islet number) compared to control, tumor burden was significantly reduced ($P < 0.05$) (Figure 5C), suggesting that tumor growth is more sensitive to reduced VEGF dose than is angiogenic switching in progenitor lesions or initial formation of small solid tumors. Of course, an alternative interpretation is that the tumor development pathway is merely de-

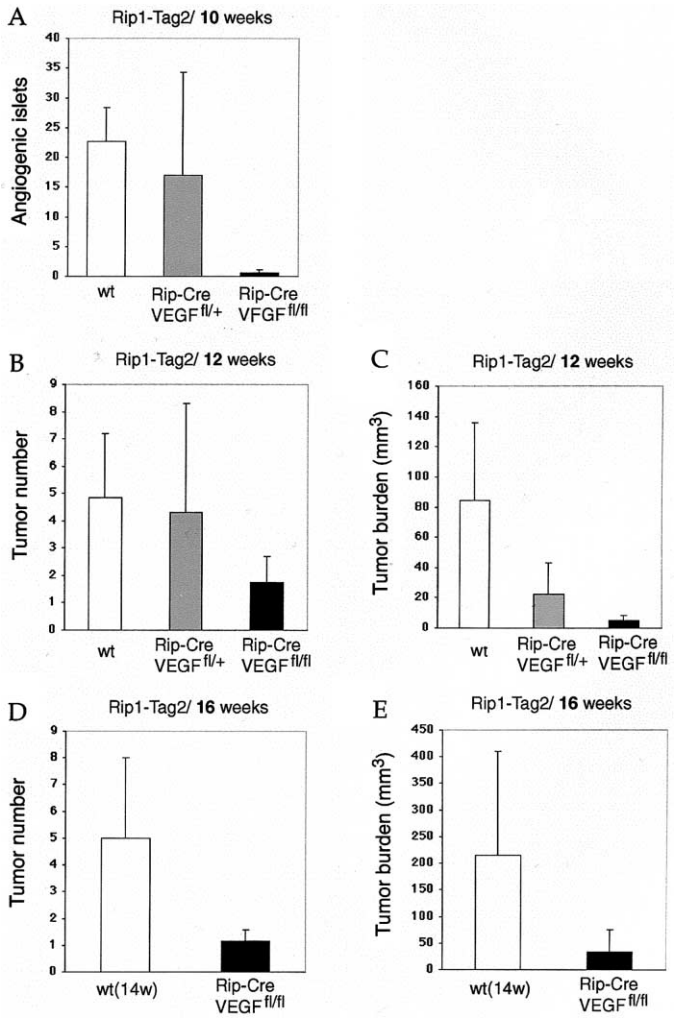


**Figure 5.** VEGF-A is instrumental in angiogenic switching and tumor growth

**A:** The incidence of angiogenic islets is compared at 10 weeks of age, when about 10% of Rip1-Tag2 islets have switched on angiogenesis. **B:** The number of tumors was determined at 12 weeks of age, comparing Rip1-Tag2/Cre;*Vegf* $^{+/+}$, Rip1-Tag2/Cre;*Vegf* $^{fl/+}$, and Rip1-Tag2/Cre;*Vegf* $^{fl/fl}$ mice. **C:** Tumor burden at 12 weeks of age is presented. **D:** Comparing the number of tumors at 14 weeks in Rip1-Tag2/Cre;*Vegf* $^{+/+}$ with that at 16 weeks of age in Rip1-Tag2/Cre;*Vegf* $^{fl/fl}$ mice. (The wt RIP1-Tag2 mice die at 14 weeks, while the Rip1-Tag2/Cre;*Vegf* $^{fl/fl}$ mice live longer, allowing for possible new tumor formation and continuing tumor growth). **E:** Tumor burden is compared at 14 weeks of age for Rip1-Tag2/Cre;*Vegf* $^{+/+}$ mice and 16 weeks of age for Rip1-Tag2/Cre;*Vegf* $^{fl/fl}$ mice.

layed, such that a similar number of tumors would eventually form.

To assess the latter possibility, that lack of VEGF-A function was merely delaying the tumor development pathway at all stages, we assessed tumor number and tumor burden at 16 weeks of age, two weeks on average after the mice with wt VEGF alleles died (Figures 5D and 5E). This analysis was afforded by the observation that RIP1-Tag2/Cre;*Vegf* $^{fl/fl}$ animals survived longer than controls. Sixteen week old RIP1-Tag2/Cre;*Vegf* $^{fl/fl}$ ($n = 6$) mice exhibited a 5-fold reduction in tumor number ($P < 0.05$), and a 6-fold reduction in tumor burden ($P < 0.05$) compared to the control mice ($n = 5$) at their end stage of 14 weeks of age. Remarkably, there was no significant increase in tumor number at 16 weeks from that observed at 12 weeks. Thus, both formation and growth of solid tumors were not just temporally delayed, but rather were significantly impaired by the absence of VEGF-A.

Three classes of tumor were revealed in RIP1-Tag2/Cre;*Vegf* $^{fl/fl}$ mice by gross pathology and subsequent histological analysis: (1) solid tumors similar in appearance to tumors in wt mice (red in color); (2) soft tumor masses that were black in color; and (3) small tumor lesions detectable only microscopically. The existence of such disparate lesions raised a question: was the VEGF gene deleted in all three classes? To assess the occurrence of Cre mediated recombination that converted *Vegf* $^{fl/fl}$ alleles into deleted *Vegf* $^{-/-}$ alleles, tumor DNA from class 1 and 2 tumors (which can be easily identified and isolated by dissection of the pancreas) was prepared and analyzed using a PCR-based assay. Six independent tumors from three RIP1-Tag2/Cre; *Vegf* $^{fl/fl}$ mice were examined; 4 out of 6 tumors had no detectable recombination. Importantly, these tumors were of the class 1 type, being relatively large, bright red, and solid. Histological analysis of the class 1 tumors having an intact, functional floxed VEGF allele indicated they were morphologically indistinguishable from wt RIP1-Tag2 and RIP1-Tag2/Cre;*Vegf* $^{+/+}$ tumors (Figures 6A and 6C); moreover, the class 1 tumors had equivalent vessel densities to control tumors, as assessed by CD31 staining (Figures 6B and 6D). No Cre immunoreactivity was observed in class 1 tumors with an intact VEGF allele (data not shown), suggesting that the RIP-Cre transgene was transcriptionally silenced, mutated, or deleted entirely. These data are consistent with prior observations that only ~85% of the β cells in mice of the particular RIP-Cre line used in this study exhibited recombination of several other floxed gene alleles and "reporter" constructs (Gannon et al., 2000). Our VEGF immunostaining of pancreatic sections from RIP-Cre;*Vegf* $^{+/+}$ mice also revealed a small number of Cre negative but VEGF positive cells, which could well be the progenitors of the class 1 "escapee" tumors.

The class 2 tumors evidenced recombinational deletion of both floxed VEGF alleles (Figure 6) and a morphology never observed in wt RIP1-Tag2 or in RIP1-Tag2/Cre;*Vegf* $^{+/+}$ control mice. The class 2 tumors were essentially hollow, with a thin shell of viable tumor cells at the periphery and a core filled with red blood cells (Figure 6E). Although RIP1-Tag2 tumors are hemorrhagic and have multiple blood islands, these islands never fuse to form such large hollow structures. The hollow tumor core could result from necrosis or massive apoptosis as a consequence of poor oxygen and nutrient supply, resulting from a dysfunctional vasculature. Blood vessels were infrequently observed within the shells of viable tumor cells at the periphery of the class 2 tumors, and more often were evident at the interface of the surrounding exocrine tissue (Figure 6F), perhaps representing co-option of preexisting normal pancreatic vessels by the tumor cells (Holash et al., 1999a). The thickness from the outer edge to the inner edge of the viable ring of tumor cells was typically ~100 μm, about the diffusion limit of oxygen from those peripheral vessels.

The class 3 tumors were smaller than the class 1 and 2 tumors (less than 2 mm) and could only be detected microscopically. However, they were very similar in morphology to the class 2 tumors, as determined by both H&E staining and lectin perfusion (Figures 7B, 7C, 7E, and 7F). Like the macroscopic class 2 tumors, these lesions had avascular cores and often

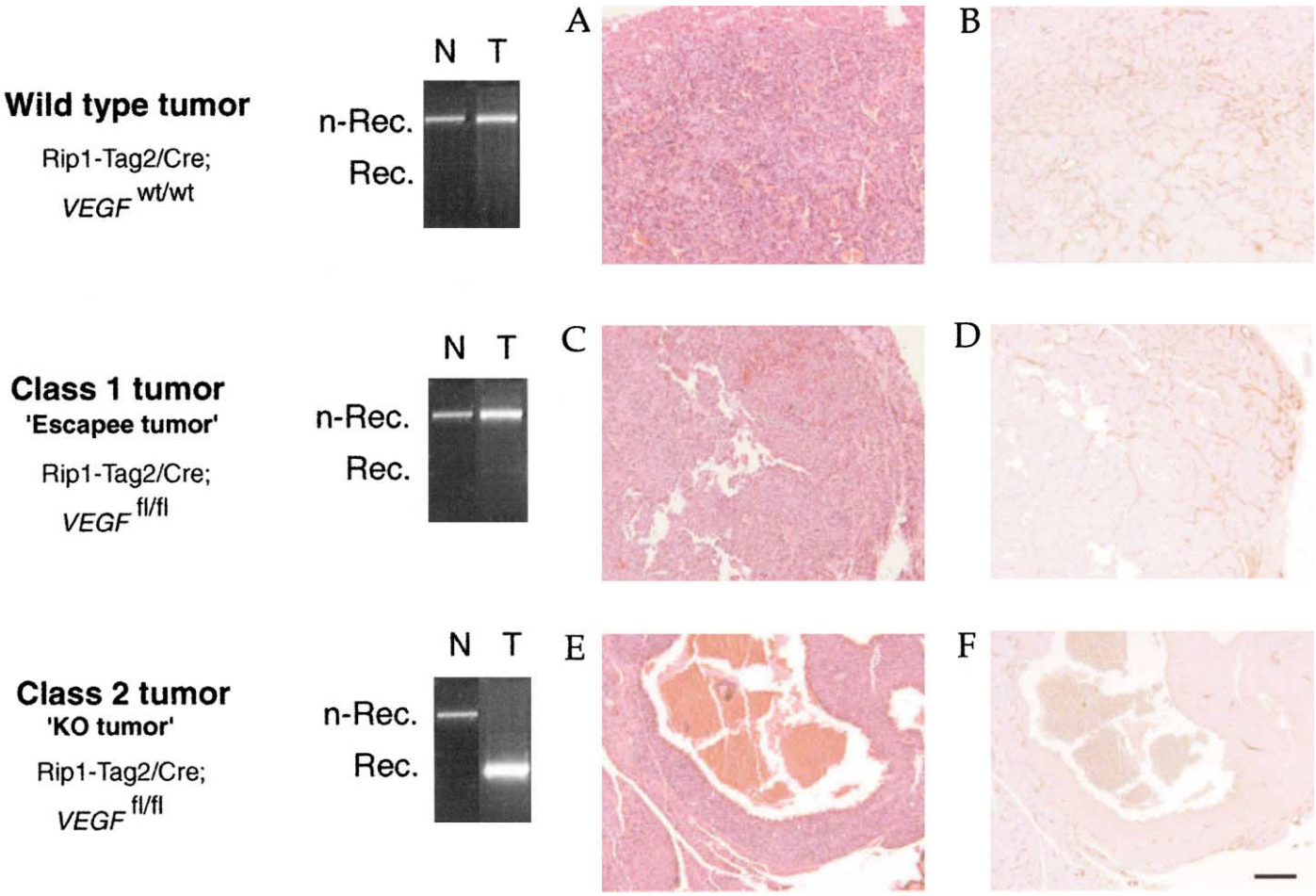


**Figure 6.** The exceptional large, well-vascularized tumors in Rip1-Tag2;Rip-Cre;Vegf$^{fl/fl}$ mice retain VEGF-A expression

The first column presents the germline genotype as determined by PCR analysis of tail-derived genomic DNA. The second column presents the data on tumor genotype (Rec = recombination of the floxed VEGF allele; n-Rec = nonrecombination of the floxed VEGF allele), as determined by PCR analysis of genomic DNA from liver (N) and tumor (T). The third and fourth columns represent H&E and CD31 staining of adjacent serial sections, respectively. **A** and **B:** A wt (Class 1) tumor exhibiting a dense, uniform vasculature that developed in a Rip1-Tag2/Cre;*Vegf*$^{+/+}$ control mouse (i.e., one that lacked floxed VEGF alleles). **C** and **D:** A Class 1 tumor from a Rip1-Tag2/Cre;*Vegf*$^{fl/fl}$ mouse in which the VEGF-flox alleles were not recombined, allowing normal VEGF expression. **E** and **F:** A markedly distinct tumor from a Rip1-Tag2/Cre;*Vegf*$^{fl/fl}$ mouse in which the VEGF floxed alleles appear to be completely recombined. H&E staining reveals the hollow nature of these (Class 2) tumors, and CD31 staining indicates that the vessels are largely restricted to the tumor perimeter. Scale bar, 100 μm.

exhibited a "hollow" tumor phenotype (Figure 7F), even in tumor lesions less than .5 mm in diameter (Figure 7C). The vessel density was highest at the periphery of these lesions, again suggesting that the growing tumor may co-opt the neighboring vessels of the surrounding exocrine pancreas. Other microscopic lesions lacked hollow cores but nevertheless exhibited reduced vessel density (Figure 7E) compared to lesions of the same size in Rip1-Tag2 control mice (Figure 7D). All tumors $>$ 2 mm in diameter were either highly vascularized (VEGF-A$^{+}$) class 1 or hollow, poorly vascularized (VEGF null) class 2 tumors.

## Discussion

An extensive literature has documented the involvement of ligand/receptor signaling circuits in both physiological and pathological angiogenesis. Most of these circuits are composed of ligand and receptor families whose members have both independent and overlapping functions. The challenge is to ascertain which of these molecules and signaling circuits govern angiogenesis in particular situations. Mouse models represent a powerful tool to address this issue, since angiogenic pathologies can be induced, and candidate genes genetically ablated to assess the consequences of their absence, as we have illustrated herein.

VEGF signaling has been clearly implicated in angiogenesis and tumorigenesis in Rip1-Tag2 mice: a soluble VEGFR-1 receptor impairs tumor angiogenesis and tumor growth (Compagni et al., 2000), as does pharmacological inhibition of VEGF-R2 (Bergers et al., 1999). Furthermore, ectopic overexpression of VEGF-A via a RIP-VEGF transgene in the context of RIP-Tag tumorigenesis enhances angiogenic switching and tumor growth (Gannon et al., 2002). Now we have clearly shown that among the 5 VEGF-receptor ligand genes found to be expressed in normal islets, VEGF-A itself is profoundly important not only for angiogenic switching, but also for tumor formation and tumor growth in this model of β cell carcinogenesis. The tissue specific

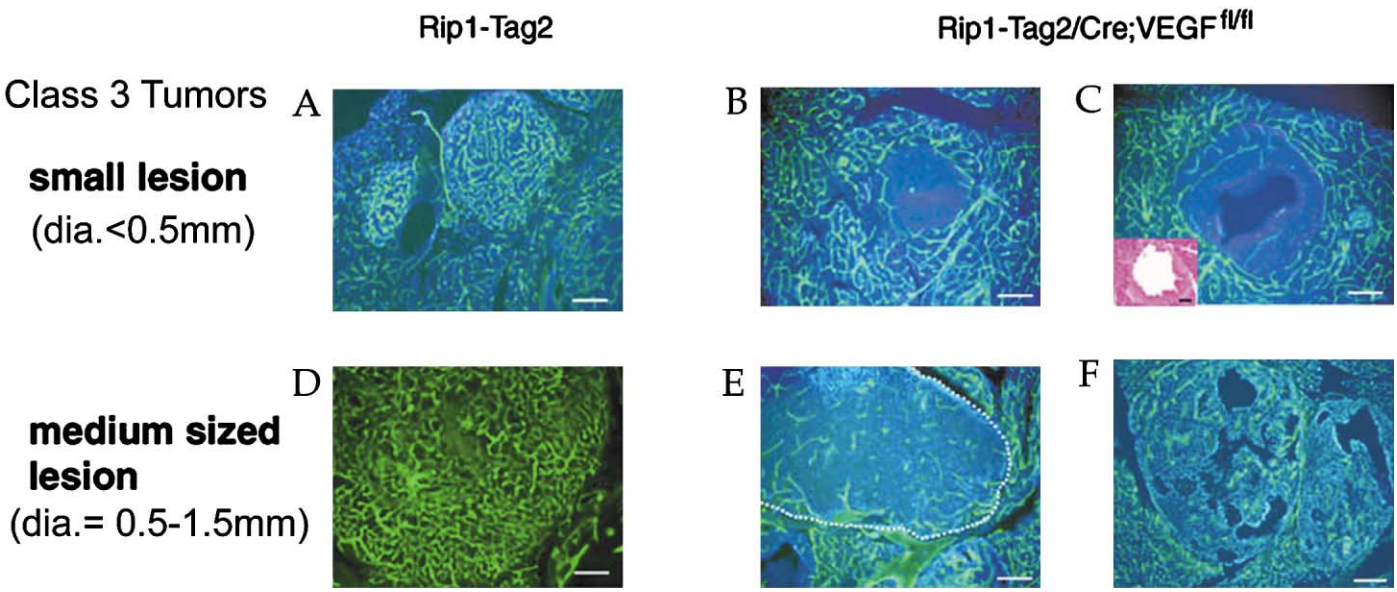


**Figure 7.** Lectin perfusion reveals an impaired vasculature in the microscopic tumor lesions of Rip1-Tag2/Cre;Vegf $^{fl/fl}$ mice

All panels visualize the vascular density and morphology of microscopic Rip1-Tag2 tumors by lectin staining. **A:** A small, microscopic (nascent) tumor lesion (less than .5 mm in diameter) from a control Rip1-Tag2/Cre;*Vegf* $^{+/+}$ mouse. **B:** In a Rip1-Tag2/Cre;*Vegf* $^{fl/fl}$ pancreas, vascular density was dramatically decreased in the core of similarly sized nascent tumors, with some showing nearly complete absence of blood vessels. **C:** In many of these microscopic tumor lesions, the hollow tumor phenotype was also evident. Inset, H&E staining of a hollow islet tumor. **D:** A typical, medium sized microscopic tumor (.5 mm to 1.5 mm in diameter) in a control Rip1-Tag2/Cre;*Vegf* $^{+/+}$ mouse, which is well vascularized and not hollow. **E:** A similarly sized Rip1-Tag2/Cre;*Vegf* $^{fl/fl}$ tumor, in which vessel density is significantly reduced. **F:** Most microscopic tumors in Rip1-Tag2/Cre;*Vegf* mice exhibit a "hollow" tumor phenotype. Scale bar, 100 μm.

knockout of VEGF-A severely impairs angiogenic switching in progenitor hyperplastic and dysplastic lesions, as well as their progression to solid tumors. Importantly, there is no evidence of alternative compensatory pathways that can substitute for VEGF-A deficiency. The proof here is in the exception: robust solid tumors are observed, but these are infrequent "escapees" from Cre-mediated deletion that manage to retain intact VEGF alleles. We have not observed robust tumors that are VEGF null, which would be indicative of an alternative compensatory pathway. This is remarkable, since normal and neoplastic islets express multiple angiogenic growth factor genes, including 10–12 members of the FGF family (Christofori and Luef, 1997; Compagni et al., 2000; Hart et al., 2000; J. Joyce and D.H., unpublished data) in addition to all five members of the VEGF family. Among the candidate FGFs, ablation of a perennial candidate, FGF-1, via crosses to FGF-1 knockout mice had no impact on angiogenic switching or tumor growth (D.H., M. Singh, et al., unpublished data).

The dramatic impact of the VEGF-A gene knockout on the tumor phenotype naturally raises the question of whether the effects are wholly consequential to vascular dysfunction. Indeed, it is now becoming apparent that the VEGF receptors are not strictly endothelial cell specific in their expression, and there is evidence for autocrine VEGF signaling via VEGF receptors expressed in certain tumor cell lines. For example, coexpression of VEGF-A, VEGF-R1, and VEGF-R2 has been detected in the tumor cells of primary pancreatic ductal adenocarcinomas (PDAC) and in cultured PDAC tumor cell lines (Itakura et al., 2000; Luo et al., 2001); the growth of PDAC cell lines could be attenuated when transfected with antisense VEGF-A or enhanced when exposed to exogenous VEGF-A. Might RIP-Tag tumor-derived VEGF-A function in a similar autocrine loop? An accumulation of evidence suggests that VEGF is not acting as an autocrine tumor growth factor for islet carcinogenesis: (1) soluble VEGF-R1 delivered by an adenovirus vector is a potent inhibitor of RIP-Tag tumor growth in vivo, but has no effect on the growth of RIP-Tag tumor cell lines (βTC) in culture (Compagni et al., 2000); (2) forced overexpression of VEGF-$A_{165}$ via a RIP-VEGF transgene accelerates the onset of RIP-Tag tumor angiogenesis, but has no effect on tumor cell proliferation or apoptosis (Gannon et al., 2002); (3) in situ hybridization and immunostaining analysis of both normal and RIP-Tag pancreas indicates that VEGF-R1/R2 expression is detectable only in the islet vasculature (Bergers et al., 2000; Christofori et al., 1995; Lammert et al., 2001); and (4) expression of the key signaling receptor, VEGF-R2, was not detected by RT-PCR analysis of 5 independent islet tumor-derived (βTC) cell lines, whereas VEGF-R1 and VEGF-R3 mRNA were detectable, but only in a subset of these same tumor cell lines, and at very low levels (J.H.H., unpublished data). Furthermore, when primary tumors were separated into constituent cell types by flow cytometry, real-time quantitative RT-PCR analysis of mRNA revealed that VEGF-R2 and R1 were expressed at 40–50 fold higher levels in the endothelial cell fraction versus the other highly purified (but not pure) cell fractions (D.H., N. Meyer-Morse, et al., unpublished data). Collectively, the evidence clearly suggests that VEGF-A functions as a modulator of angiogenesis and not as an autocrine growth factor in this setting. Engineering a β cell specific "KO" of VEGF-R1/2 in the context of RIP-Tag tumorigenesis would definitively test whether VEGF-A has some subtle autocrine contribution to tumor growth.

The results of ablating VEGF-A have several implications.

The first involves nonredundancy and lack of functional compensation amongst the family of VEGF ligand genes expressed in this pathway. Quantitative PCR analysis has revealed that VEGF-B, -C, -D, and PLGF are all expressed in normal islets and throughout RIP1-Tag2 tumorigenesis. The results indicate that no other member of the VEGF gene family can substitute for lack of VEGF-A function insofar as they are expressed during islet tumorigenesis (Figure 2). Some of us have previously reported apparent compensatory upregulation of VEGF-A and PLGF following treatment of an orthotopic tumor with anti-VEGF-A therapy (Gerber et al., 2000). In the RIP1-Tag2 model, the absence of compensation could result from a lack of sufficient transcriptional upregulation (Gerber et al., 2000), or from a lack of ligand mobilization by proteolysis as occurs for VEGF-A (Bergers et al., 2000), or from an absence of functional overlap in signaling. Certainly further studies on protein levels, isoforms, and bioavailability of VEGF-B, -C, -D, and PlGF are warranted, both in the wt and VEGF-A/null situations. Indeed, it would not be surprising to find that another VEGF ligand has an important role in this tumorigenesis pathway, functioning as a "cofactor" or potentiator of VEGF-A signaling that is not itself sufficient to "trip" the angiogenic switch or sustain tumor angiogenesis in the absence of VEGF-A. Interestingly, it has been recently reported that overexpression of VEGF-C in the islet β cells via a RIP-VEGF-C transgene induces peri-islet lymphatic vessels but has no discernable effect on intra-islet blood vessels (Mandriota et al., 2001). Likewise, in the context of RIP1-Tag2 tumorigenesis, VEGF-C overexpression did not increase intra-tumoral vascularity or enhance tumor growth; instead, peri-tumoral lymphatic vessels induced by VEGF-C facilitated metastases to the draining mesenteric lymph nodes (Mandriota et al., 2001). This result argues that VEGF-C functions primarily to regulate lymphangiogenesis and not tumor blood vessel growth in the RIP-Tag model, a hypothesis that awaits evaluation via a more definitive loss-of-function study. Likewise, the systematic genetic ablation of PLGF, VEGF-B, and VEGF-D should reveal contributions by these molecules to this prototypical pathway of tumorigenesis.

A growing body of data suggests that carcinoma cells can invade into normal tissue, enveloping, or co-opting, quiescent blood vessels to sustain their survival and proliferation (Holash et al., 1999a, 1999b; Pezzella et al., 1997). Apparent vessel co-option has been observed during histopathological analysis of human tumors (Pezzella et al., 1997) and tumor xenotransplant models (Holash et al., 1999a; Kunkel et al., 2001; Rubenstein et al., 2000), and there is reason to suspect that co-option has the potential to predominate when angiogenesis is suppressed, as a consequence of tissue microenvironment or pharmacological inhibition. Indeed, we suspect that co-option is involved in the survival of a thin rim of tumors cells at the periphery of the hollow, type II/III islet tumors, where the tumor cells appear to be in close apposition to preexisting vessels of the surrounding exocrine pancreas. It follows that the RIP-Tag/VEGF null model could prove useful for studying vessel co-option and preclinical testing of treatment strategies that might abrogate it.

### Implications for human cancer therapy

In summary, our genetic analysis of VEGF-A gene function during islet tumorigenesis encourages the ongoing development of pharmacological inhibitors of VEGF signaling in general, and of the VEGF-A ligand in particular. It is, however, important to recognize that the VEGF gene knockout was present throughout tumorigenesis in this study, and thus most accurately mimics a completely efficacious cancer prevention trial targeting VEGF-A. Notably, preclinical trails in the RIP-Tag model of a pharmacological inhibitor of VEGF-R2 (SU5416) revealed similar reductions in the initial induction of angiogenesis (angiogenic switching frequency) in the still quiescent vasculature of hyperplastic/dysplastic lesions, and similar restrictions of nascent tumor growth (Bergers et al., 2000); in both trials, treatment was initiated early in disease progression. Thus, both the gene knockout and the "pharmacological knockout" of VEGF-A signaling in the RIP-Tag model predict that VEGF inhibitors could have value as stand-alone agents in pharmacological prevention of incipient neoplasia. By contrast, the VEGF-R inhibitor did not produce an objective response (tumor regression) when it was used to treat large, well-established islet tumors in RIP1-Tag2 mice (D.H., G. Bergers, et al., unpublished data), not unlike several other angiogenesis inhibitors (Bergers et al., 1999). Similarly, the ongoing clinical trials of agents that inhibit VEGF-A or its receptors against late stage human tumors do not appear to be producing dramatic results. While most of the definitive trials are still in progress and hence unpublished, it is pertinent to note the case of SU5416, which has recently been withdrawn from Phase III trials, a decision motivated in part a lack of objective responses against late stage colon cancer (Press Release, Pharmacia Corp., Feb. 8, 2002; http://www.pharmacia.com/News/NewsDisplay.asp?PR=267). One explanation of these disappointing results with SU5416 in both mouse and human trials is that late stage tumors can activate additional angiogenic regulatory circuits which function in concert with or independent of VEGF-A/VEGF-R2 signaling, reducing their VEGF dependence. If so, one must infer that the VEGF-A/null tumors described above never achieve this late stage of progression where VEGF-A activity is less singular. A second, quite plausible explanation is that tumor angiogenesis remains highly dependent on VEGF-A signaling in late stage cancers, but the current formulations of VEGF-A and VEGF-receptor inhibitors do not achieve complete blockade of VEGF-A signaling inside well-established, solid tumors. If so, then future improvements in bioavailability and pharmacodynamics of VEGF-A/VEGF-R inhibitors in cancerous lesions could affect a complete pharmacological knockout of VEGF-A function, enabling such drugs to achieve results analogous to those we report for the VEGF-A gene knockout. Nevertheless, it seems likely that other angiogenic signaling circuits make important qualitative or quantitative contributions to the vascularization of tumors as they progress; indeed, FGF signaling is implicated from therapeutic trials with a functional inhibitor in the RIP-Tag model (Compagni et al., 2000). Looking forward, combinatoric inhibition both of VEGF-A signaling and of those angiogenic regulatory circuits that enhance or complement VEGF in particular tumor types, perhaps along with blockade of the invasive program that co-opts normal vessels, could present a powerful strategy for treating human cancers.

### Experimental procedures

#### Real-time quantitative RT-PCR of VEGF family member expression

Total RNA from normal, nontransgenic islets and from angiogenic islets and tumors from RIP1-Tag2 mice was isolated using the STAT 60 method (TEL-TEST "B," Friendswood, TX) and purified on RNeasy Quick spin columns

(Qiagen, Valencia, CA). Probe primer sequences for all genes except VEGF-D and real-time RT-PCR conditions, as well as methods applied for data analysis, were as described previously (Gerber et al., 2000). A total of 100 ng of total RNA was used per RT-PCR reaction. RNA levels were standardized to the probe/primer set for murine GAPDH. For linear regression, total RNA from adult mouse liver (Clonetech, Palo Alto, CA) was used. Oligo sequences for RT-PCR analysis of murine VEGF-D were: probe, (MMVEGFD.1326.T) ACATTTCCATGCAATGGCGGCT; forward primer, (MMVEGFD.1302.F) TTGACCTAGTGTCATGGTAAAGC; and reverse primer, (MMVEGFD.1369.R) TCAGTGAACTGGGGAATCAC.

**Generation of Rip1-Tag2/Cre;*Vegf*$^{fl/fl}$**

The generation and phenotypic characterization of Rip1-Tag2 transgenic mice (Hanahan, 1985), Rip-Cre transgenic mice (Postic et al., 1999), and VEGF floxed mice (Gerber et al., 1999) have been reported. To minimize the effects of genetic modifiers on the tumor phenotype, all mice were backcrossed to C57BL/6J for a minimum of 4 generations (N4) prior to initiating the crosses to generate the compound transgenic/KO mice: Rip1-Tag2 (N35), RIP-Cre (N15), and VEGF floxed (N4). We mated *Vegf*$^{fl/+}$ mice with Rip-Cre to generate RIP-Cre;*Vegf*$^{fl/+}$, and in parallel mated *Vegf*$^{fl/+}$ mice with Rip1-Tag2 to obtain RIP1-Tag2;*Vegf*$^{fl/+}$ mice. Mating of these compound heterozygous offspring yielded various genotypes, including Rip1-Tag2/Cre;*Vegf*$^{+/+}$, Rip1-Tag2/Cre;*Vegf*$^{fl/+}$, and Rip1-Tag2/Cre;*Vegf*$^{fl/fl}$. These offspring were used in crosses to generate the desired genotypes.

**Assessment of angiogenic islets, tumor burden, and tumor frequency**

Angiogenic islets were isolated by retrograde perfusion following collagenase P digestion, and counted under a dissecting microscope. Angiogenic islets were identified as those that exhibited a reddish patch or patches in a white nodular background. The visual scoring scheme was confirmed by histology as described (Parangi et al., 1995). Tumors were microdissected from freshly excised pancreases. Tumor volumes were measured with calipers, and the formula [volume $= 0.52 \times (\text{width})^2 \times$ length] for approximating the volume of spheroid was applied. Tumor burden per mouse equals the sum of the tumor volumes of every mouse. Comparisons between groups were analyzed by t test (two tailed) or ANOVA for experiments with more than two subgroups. P values less than 0.05 were considered statistically significant.

**Histological analysis**

For immunohistochemistry, excised pancreas was fixed with neutral buffered formalin or 4% paraformaldehyde (PFA) at 4°C overnight. The tissues were then processed and embedded in paraffin, or in OCT compound for frozen sections, and processed as described (Bergers et al., 1999). Antibodies for CD31 (diluted 1:50) and VEGF (diluted 1:400) were purchased from Pharmingen (San Diego, CA) and Neomarkers (Fremont, CA), respectively, and immunohistochemistry carried out as described (Bergers et al., 2000), except that all primary antibody reaction products were visualized with respective biotinylated secondary antibodies and then incubated with ABC reagent (Vectastain, Vector, Buringame, CA), and visualized with peroxidase substrate kit (NovaRED, Vector).

**Lectin perfusion and vascular staining**

Mice were anesthetized with an intraperitineal (IP) injection of nemubutal. Flouroscein-labeled lectin (Lycopersicon Esculentum, Vector), was injected into tail vein (1 mg/ml solution/0.1 ml/mouse) and allowed to circulate for 3 min, after which the mice were heart perfused with 2% PFA for 3 min. The pancreas was excised and immersion-fixed in 4% PFA for 4 to 16 hr at 4°C. Post fixation, pancreata were immersed in 30% sucrose as a cryoprotectant, after which the tissue was embedded in OCT compound. The block was sectioned at 60 μm thickness and collected on Fisher brand Superfrost/Plus microscope slides. Sections were rinsed in PBS and covered with Vectershield w/DAPI (Vector) to visualize nuclei. The slides were observed under the fluorescent microscope (Zeiss, Thoruwood, New York) with 10× objective and the images were captured with a CCD camera (Hamamatsu Photonics, Bridgewater, New Jersey) with Openlab software (Improvision Lexington, Massachusetts).

**Recombination assay**

The primer set was designed to flank both of the engineered loxP sites; following amplification, the product generated from the nonrecombined allele was about 1800 bp, while the recombined allele was about 200 bp. Primer sequences were VEGF419F (5′-CCTGGCCCTCAAGTACACCTT-3′) and VEGFc5R2 (5′-ACATCTGCTGTGCTGTAGGAAG-3′).To assess recombinational deletion of VEGF-A in tumors, a segment of the tumor tissue was excised (prior to embedding the remainder for histopathological analyses), from which DNA was extracted, and analyzed for recombination using the PCR assay.

**Acknowledgments**

We wish to thank Zena Werb, Gerhard Christofori, and Richard Hynes for comments on the manuscript. M.I. was supported in part by the Toyobo Bioscience Foundation. The authors also acknowledge Taichi Ezaki and Shinichi Morikawa for technical advice regarding lectin perfusion. We thank Mark Magnuson (Vanderbilt University) for the RIP-Cre mice. This research was supported by grants from the N.C.I. to D.H.

Received: January 28, 2002
Revised: March 1, 2002

**References**

Bergers, G., Javaherian, K., Lo, K.M., Folkman, J., and Hanahan, D. (1999). Effects of angiogenesis inhibitors on multistage carcinogenesis in mice. Science *284*, 808–812.

Bergers, G., Brekken, R., McMahon, G., Vu, T.H., Itoh, T., Tamaki, K., Tanzawa, K., Thorpe, P., Itohara, S., Werb, Z., and Hanahan, D. (2000). Matrix metalloproteinase-9 triggers the angiogenic switch during carcinogenesis. Nat. Cell Biol. *2*, 737–744.

Carmeliet, P., Ferreira, V., Breier, G., Pollefeyt, S., Kieckens, L., Gertsenstein, M., Fahrig, M., Vandenhoeck, A., Harpal, K., Eberhardt, C., et al. (1996). Abnormal blood vessel development and lethality in embryos lacking a single VEGF allele. Nature *380*, 435–439.

Christofori, G., and Luef, S. (1997). Novel forms of acidic fibroblast growthfactor-1 are constitutively exported by b tumor cell lines independent from conventional secretion and apoptosis. Angiogenesis *1*, 55–70.

Christofori, G., Naik, P., and Hanahan, D. (1995). Vascular endothelial growth factor and its receptors, flt-1 and flk-1, are expressed in normal pancreatic islets and throughout islet cell tumorigenesis. Mol. Endocrinol. *9*, 1760–1770.

Compagni, A., Wilgenbus, P., Impagnatiello, M.A., Cotten, M., and Christofori, G. (2000). Fibroblast growth factors are required for efficient tumor angiogenesis. Cancer Res. *60*, 7163–7169.

Ferrara, N. (1999). Molecular and biological properties of vascular endothelial growth factor. J. Mol. Med. *77*, 527–543.

Ferrara, N., Carver-Moore, K., Chen, H., Dowd, M., Lu, L., O'Shea, K.S., Powell-Braxton, L., Hillan, K.J., and Moore, M.W. (1996). Heterozygous embryonic lethality induced by targeted inactivation of the VEGF gene. Nature *380*, 439–442.

Folkman, J., Watson, K., Ingber, D., and Hanahan, D. (1989). Induction of angiogenesis during the transition from hyperplasia to neoplasia. Nature *339*, 58–61.

Gannon, M., Shiota, C., Postic, C., Wright, C.V., and Magnuson, M. (2000). Analysis of the Cre-mediated recombination driven by rat insulin promoter in embryonic and adult mouse pancreas. Genesis *26*, 139–142.

Gannon, G., Mandriota, S.J., Cui, L., Baetens, D., Pepper, M.S., and Christofori, G. (2002). Overexpression of vascular endothelial growth factor-A165 enhances tumor angiogenesis but not metastasis during beta-cell carcinogenesis. Cancer Res. *62*, 603–608.

Gerber, H.P., Hillan, K.J., Ryan, A.M., Kowalski, J., Keller, G.A., Rangell, L., Wright, B.D., Radtke, F., Aguet, M., and Ferrara, N. (1999). VEGF is required for growth and survival in neonatal mice. Development *126*, 1149–1159.

Gerber, H.P., Kowalski, J., Sherman, D., Eberhard, D.A., and Ferrara, N. (2000). Complete inhibition of rhabdomyosarcoma xenograft growth and

neovascularization requires blockade of both tumor and host vascular endothelial growth factor. Cancer Res. *60*, 6253–6258.

Hanahan, D. (1985). Heritable formation of pancreatic beta-cell tumours in transgenic mice expressing recombinant insulin/simian virus 40 oncogenes. Nature *315*, 115–122.

Hanahan, D., and Folkman, J. (1996). Patterns and emerging mechanisms of the angiogenic switch during tumorigenesis. Cell *86*, 353–364.

Hanahan, D., and Weinberg, R.A. (2000). The hallmarks of cancer. Cell *100*, 57–70.

Hart, A.W., Baeza, N., Apelqvist, A., and Edlund, H. (2000). Attenuation of FGF signalling in mouse beta-cells leads to diabetes. Nature *408*, 864–868.

Holash, J., Maisonpierre, P.C., Compton, D., Boland, P., Alexander, C.R., Zagzag, D., Yancopoulos, G.D., and Wiegand, S.J. (1999a). Vessel cooption, regression, and growth in tumors mediated by angiopoietins and VEGF. Science *284*, 1994–1998.

Holash, J., Wiegand, S.J., and Yancopoulos, G.D. (1999b). New model of tumor angiogenesis: dynamic balance between vessel regression and growth mediated by angiopoietins and VEGF. Oncogene *18*, 5356–5362.

Itakura, J., Ishiwata, T., Shen, B., Kornmann, M., and Korc, M. (2000). Concomitant over-expression of vascular endothelial growth factor and its receptors in pancreatic cancer. Int. J. Cancer *85*, 27–34.

Kulkarni, R.N., Bruning, J.C., Winnay, J.N., Postic, C., Magnuson, M.A., and Kahn, C.R. (1999). Tissue-specific knockout of the insulin receptor in pancreatic beta cells creates an insulin secretory defect similar to that in type 2 diabetes. Cell *96*, 329–339.

Kunkel, P., Ulbricht, U., Bohlen, P., Brockmann, M.A., Fillbrandt, R., Stavrou, D., Westphal, M., and Lamszus, K. (2001). Inhibition of glioma angiogenesis and growth in vivo by systemic treatment with a monoclonal antibody against vascular endothelial growth factor receptor-2. Cancer Res. *61*, 6624–6628.

Lammert, E., Cleaver, O., and Melton, D. (2001). Induction of pancreatic differentiation by signals from blood vessels. Science *294*, 564–567.

Luo, J., Guo, P., Matsuda, K., Truong, N., Lee, A., Chun, C., Cheng, S.Y., and Korc, M. (2001). Pancreatic cancer cell-derived vascular endothelial growth factor is biologically active in vitro and enhances tumorigenicity in vivo. Int. J. Cancer *92*, 361–369.

Mandriota, S.J., Jussila, L., Jeltsch, M., Compagni, A., Baetens, D., Prevo, R., Banerji, S., Huarte, J., Montesano, R., Jackson, D.G., et al. (2001). Vascular endothelial growth factor-C-mediated lymphangiogenesis promotes tumour metastasis. EMBO J. *20*, 672–682.

Parangi, S., Dietrich, W., Christofori, G., Lander, E.S., and Hanahan, D. (1995). Tumor suppressor loci on mouse chromosomes 9 and 16 are lost at distinct stages of tumorigenesis in a transgenic model of islet cell carcinoma. Cancer Res. *55*, 6071–6076.

Pezzella, F., Pastorino, U., Tagliabue, E., Andreola, S., Sozzi, G., Gasparini, G., Menard, S., Gatter, K.C., Harris, A.L., Fox, S., et al. (1997). Non-small-cell lung carcinoma tumor growth without morphological evidence of neoangiogenesis. Am. J. Pathol. *151*, 1417–1423.

Postic, C., Shiota, M., Niswender, K.D., Jetton, T.L., Chen, Y., Moates, J.M., Shelton, K.D., Lindner, J., Cherrington, A.D., and Magnuson, M.A. (1999). Dual roles for glucokinase in glucose homeostasis as determined by liver and pancreatic beta cell-specific gene knock-outs using Cre recombinase. J. Biol. Chem. *274*, 305–315.

Rubenstein, J.L., Kim, J., Ozawa, T., Zhang, M., Westphal, M., Deen, D.F., and Shuman, M.A. (2000). Anti-VEGF antibody treatment of glioblastoma prolongs survival but results in increased vascular cooption. Neoplasia *2*, 306–314.

Shibuya, M., Ito, N., and Claesson-Welsh, L. (1999). Structure and function of vascular endothelial growth factor receptor-1 and -2. Curr. Top. Microbiol. Immunol. *237*, 59–83.

Vajkoczy, P., Menger, M.D., Vollmar, B., Schilling, L., Schmiedek, P., Hirth, K.P., Ullrich, A., and Fong, T.A. (1999). Inhibition of tumor growth, angiogenesis, and microcirculation by the novel Flk-1 inhibitor SU5416 as assessed by intravital multi- fluorescence videomicroscopy. Neoplasia *1*, 31–41.

Van Dyke, T., and Jacks, T. (2002). Cancer modeling in the modern era. Progress and challenges. Cell *108*, 135–144.